Halide-Ion Encapsulation by a Flexible Dicopper(II) Bis-Tren Cryptate

Valeria Amendola, Emanuela Bastianello,
Luigi Fabbrizzi,* Carlo Mangano,
Piersandro Pallavicini, Angelo Perotti,
Anna Manotti Lanfredi,* and Franco Ugozzoli

Homodimetallic complexes of bis-tren cryptands such as **1**–**3** are suitable receptors for anionic substrates. Each metal center (e.g., $\mathrm{Cu^{II}}$) is coordinated by a tren subunit according to a trigonal bipyramidal stereochemistry, thus leaving an axial site vacant and available for the coordination of an anion.

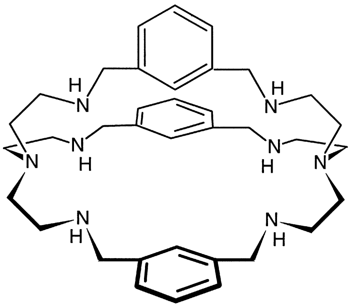

1

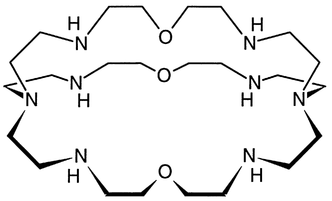

2

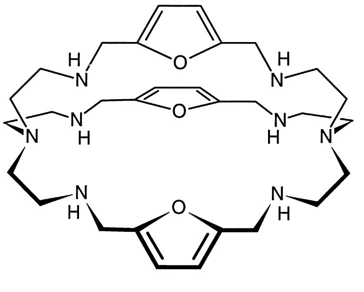

3

The dicopper(II) complex of the bis-tren cryptand **1**, which contains rigid 3,5-xylyl spacers, encapsulates ambidentate anions such as $\mathrm{N_3^-}$ and $\mathrm{NCO^-}$, and the structural details of the inclusion adducts have been determined by X-ray diffraction studies. The anion collinearly bridges the two metal centers by coordination of its terminal donor atoms.[1] Moreover, the $\log K$ values for the inclusion equilibrium in an aqueous solution buffered at pH 8 [Eq. (1)] were determined by spectrophotometric titration experiments.[2] A sharp selectivity exists that is not related to the shape of the anion, but to its "bite length", that is, the distance between the two donor atoms. In particular, the most favorable inclusion is observed with the $\mathrm{N_3^-}$ ion, which exhibits the correct bite length to position its terminal nitrogen atoms in the vacant coordination sites of the two $\mathrm{Cu^{II}}$ centers without inducing any endothermic rearrangement of the polyamine cage. Monoatomic anions such as halides are not encapsulated by the cryptate $[\mathrm{Cu_2^{II}}(\mathbf{1})]^{4+}$, even if added in a large excess. Failure to include halide ions seems to be attributable to the mechanical resistence of the rigid cage framework to adjusting its cavity to the size requirements of the monoatomic guest anion. In contrast, encapsulation of chloride ions by the cryptate $[\mathrm{Cu_2^{II}}(\mathbf{2})]^{4+}$ has been hypothesized on the basis of potentiometric titration experiments carried out in the absence and presence of NaCl.[3] Inclusion of chloride ions and bridging of the two $\mathrm{Cu^{II}}$ centers should be favored by the flexible nature of the $\mathrm{CH_2CH_2OCH_2CH_2}$ spacers. Halide bridging, both in the solid state and in solution, was observed in the dicopper(II) complex of the very flexible octamine ligand *N*,*N'*,*N''*,*N'''*-tetrakis-(2-aminoethylcyclam).[4, 5]

$$[\mathrm{Cu_2^{II}}(\mathbf{1})]^{4+} + \mathrm{X^-} \rightleftharpoons [\mathrm{Cu_2^{II}}(\mathbf{1})(\mathrm{X})]^{3+} \qquad (1)$$

Among other bis-tren cryptands containing rigid spacers, we noticed the peculiar behavior of the dicopper(II) complex of **3**, in which the two tripodal tetramine subunits are linked by 2,5-dimethylfuran spacers. In particular, the complex $[\mathrm{Cu_2^{II}}(\mathbf{3})(\mathrm{OH})]^{3+}$ was isolated and structurally characterized,[6] in which an $\mathrm{OH^-}$ ion bridges the two metal centers. The $\mathrm{Cu^{II}\cdots Cu^{II}}$ distance of 3.87 Å is much smaller than that observed for the complexes $[\mathrm{Cu_2^{II}}(\mathbf{1})(\mathrm{X})]^{3+}$ ($\mathrm{X = N_3^-}$: 6.10 Å; $\mathrm{NCO^-}$: 6.18 Å). Hence, we thought that $[\mathrm{Cu_2^{II}}(\mathbf{3})]^{4+}$ might be able to encapsulate monoatomic anions of comparable or larger size and exhibit a different selectivity pattern than $[\mathrm{Cu_2^{II}}(\mathbf{1})]^{4+}$.

We first investigated the formation of the dicopper(II) cryptate of **3** in aqueous solution by carrying out potentiometric titration experiments on a solution of **3** and $\mathrm{Cu^{II}}$ in a 1:2 molar ratio (25 °C, 0.1 M $\mathrm{NaClO_4}$). The $\log K$ values for the species present at the equilibrium were calculated, and their abundance over the pH range 2–12 is illustrated in Figure 1.

Two major dimetallic species are present in the pH 4–11 region: a $[\mathrm{Cu_2^{II}L}]^{4+}$ complex in the range pH 4–7 (maximum concentration: 85 %, at pH 5; indicated in the graph by 120) and a $[\mathrm{Cu_2^{II}L(OH)}]^{3+}$ complex in the range pH 6–11 (maximum concentration: 97 %, at pH 8, indicated by 12-1). A solution adjusted to pH 8 (ca. 100 % of the complex $[\mathrm{Cu_2^{II}L(OH)}]^{3+}$), emerald green in color, displays similar spectral features ($\lambda_{\max} = 362$ nm; $\varepsilon = 6500\,\mathrm{M^{-1}\,cm^{-1}}$) to those observed for a solution of the crystalline $[\mathrm{Cu_2^{II}L(OH)}](\mathrm{ClO_4})_3$ in MeCN (360 nm, $4700\,\mathrm{M^{-1}\,cm^{-1}}$), which was structurally characterized.[7] The development of the band centered at 362 nm, pertinent to the emerald green color, was

---

[*] Prof. L. Fabbrizzi, Dr. V. Amendola, Dr. E. Bastianello, C. Mangano, Dr. P. Pallavicini, Prof. A. Perotti
Dipartimento di Chimica Generale
Università di Pavia
via Taramelli 12, 27100 Pavia (Italy)
Fax: (+39) 0382-507-328
E-mail: fabbrizz@unipv.it

Prof. A. Manotti Lanfredi, Prof. F. Ugozzoli
Dip. di Chimica Generale ed Inorganica
Chimica Analitica, Chimica Fisica, Università di Parma
Parco Area delle Scienze 17/a, 43100 Parma (Italy)
Fax: (+39) 0521-905-557
E-mail: ugoz@.unipr.it

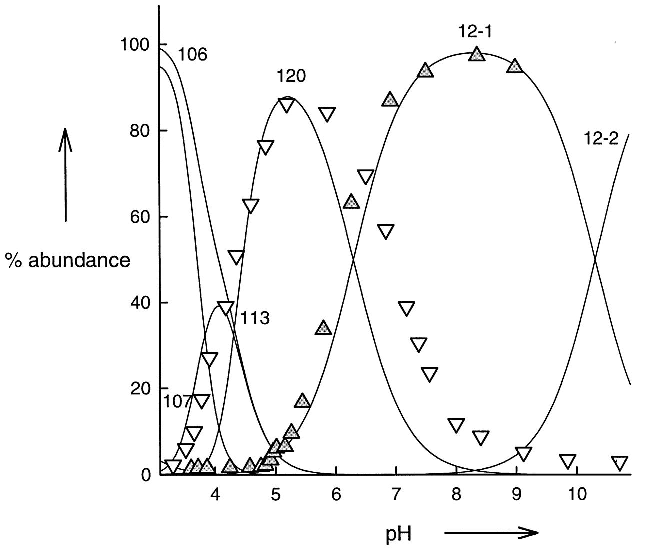

Figure 1. Percentage concentration of the species present at equilibrium in the system **3**/Cu^{II} (ligand:metal 1:2) in a 0.1 M aqueous solution of NaClO$_4$ at 25°: the figures in the triads indicate the number of molecules of **3**, Cu^{2+}, and H$^+$ contained in each species; −1 indicates the OH$^-$ ion; for example, 12 −1 symbolizes $[\mathrm{Cu}_2^{\mathrm{II}}(\mathbf{3})(\mathrm{OH})]^{3+}$. ▲ indicate the absorbance of the band centered at 362 nm (pertinent to the green complex $[\mathrm{Cu}_2^{\mathrm{II}}(\mathbf{3})(\mathrm{OH})]^{3+}$; arbitrary units; limiting value of molar absorbance is 6500 M^{-1}cm^{-1}). △ indicate the absorbance of the band centered at 410 nm, measured in the presence of a tenfold excess of Cl$^-$ (pertinent to the yellow complex $[\mathrm{Cu}_2^{\mathrm{II}}(\mathbf{3})(\mathrm{Cl})]^{3+}$; arbitrary units; limiting value of molar absorbance is 12600 M^{-1} cm^{-1}).

then monitored at varying pH by spectrophotometric titration: the molar absorbance profile superimposes well on the percentage concentration profile of the $[\mathrm{Cu}_2^{\mathrm{II}}\mathrm{L}(\mathrm{OH})]^{3+}$ species (see ▲ in Figure 1). All these results suggest that in the aqueous dicopper(II) cryptate the OH$^-$ ion is also included within the cavity. On the other hand, in the absence of coordinating anions, the intermetallic cavity in the $[\mathrm{Cu}_2^{\mathrm{II}}\mathrm{L}]^{4+}$ complex is thought to be "void" or, more realistically, occupied by water molecules or the anion of the background electrolyte, that is, ClO$_4^-$.

The binding tendencies of the dicopper(II) cryptates $[\mathrm{Cu}_2^{\mathrm{II}}\mathrm{L}]^{4+}$ and $[\mathrm{Cu}_2^{\mathrm{II}}\mathrm{L}(\mathrm{OH})]^{3+}$ towards anions were investigated by spectrophotometric titration at varying pH in the presence of the envisaged anion X$^-$. Remarkable spectral effects were observed when X$^-$ was a halide. For Cl$^-$, Br$^-$, and I$^-$ at pH > 3, the solution became bright yellow, and an intense band developed above 400 nm in the spectrum (Cl$^-$, $\lambda_{\max} = 410$; Br$^-$, 430 nm; I$^-$, 440 nm). For example, the values of the absorbance at 410 nm as a function of pH for a 10^{-3} M solution of dicopper(II) cryptate containing 10^{-2} M NaCl are shown in Figure 1 (△). The band develops in the pH range in which the empty cryptate $[\mathrm{Cu}_2^{\mathrm{II}}\mathrm{L}]^{4+}$ is present, and this suggests that in the presence of Cl$^-$ ions a strong interaction is established between the halide ion and the metal center(s). Hence, the intense absorption band should result from a $\mathrm{Cl}^- \rightarrow \mathrm{Cu}^{\mathrm{II}}$ charge-transfer transition. Similar absorbance versus pH plots were observed for solutions with 10^{-2} M bromide or iodide ions.

Yellow crystals of $[\mathrm{Cu}_2^{\mathrm{II}}(\mathbf{3})(\mathrm{Br})](\mathrm{ClO}_4)_3$ suitable for X-ray diffraction studies were obtained on slow evaporation of the bromide-containing solution adjusted to pH 5.2 (Figure 2).[8]

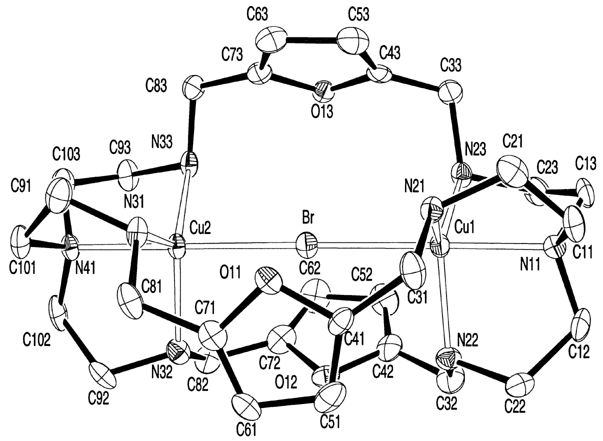

Figure 2. ORTEP plot (30% probability thermal ellipsoids) of $[\mathrm{Cu}_2^{\mathrm{II}}(\mathbf{3})(\mathrm{Br})]^{3+}$. Hydrogen atoms are omitted for clarity. Selected bond lengths [Å] and angles [°]: Cu1-Br 2.432(1), Cu2-Br 2.435(1), Cu-N11 2.048(7), Cu1-N21 2.092(7), Cu1-N22 2.096(7), Cu1-N23 2.091(8), Cu2-N41 2.046(7), Cu2-N31 2.070(7), Cu2-N32 2.131(8), Cu2-N33 2.103(7), Cu1-Cu2 4.866(2); Cu1-Br-Cu2 179.4(1), Br-Cu1-N11 179.4(2), Br-Cu2-N41 179.4(1), N21-Cu1-N22 119.0(3), N21-Cu1-N23 123.7(3), N22-Cu1-N23 115.9(3), N31-Cu2-N32 117.3(3), N31-Cu2-N33 124.8(3), N32-Cu2-N33 116.3(3).

The Br$^-$ ion is encapsulated within the cage and bridges the two metal centers. Cu1 and Cu2 exhibit a trigonal-bipyramidal geometry and are slightly displaced from the least-squares plane of the three secondary amino nitrogen atoms of each tren subunit towards the halide ion (0.145(1) and 0.157(1) Å, respectively). The Cu1 ··· Cu2 distance is 4.86 Å, and the Cu1-Br-Cu2 angle is 179.4°. Hence, the bright yellow color and the intense absorption band around 400 nm can be ascribed to the inclusion of the halide ion within the dicopper(II) cryptate. Notably, the halide inclusion complex is stable only in a restricted pH range, as indicated by the bell-shaped profile of the absorbance of $[\mathrm{Cu}_2^{\mathrm{II}}(\mathbf{3})(\mathrm{Cl})]^{3+}$ (Figure 1). The same profiles, centered at pH 5.2, were also observed for the Br$^-$ and I$^-$ derivatives. The bright yellow solution turns emerald green on increasing the pH; this indicates that the halide ion is replaced by OH$^-$. Anion replacement is fast and reversible, and the solution can be made to turn yellow and green consecutively by the sequential addition of a few drops of standard base and acid.

To quantify the binding tendencies of the dicopper(II) cryptate towards halide ions and to assess selectivity effects, a solution containing **3** and two equivalents of Cu^{II} and buffered to pH 5.2 was titrated with a standard solution of sodium halide NaX. The pale blue solution (color of the void complex) turned bright yellow on addition of X$^-$. Figure 3 shows the family of spectra recorded during the titration with chloride ion. The titration profile in the inset corresponds to the formation of a 1:1 inclusion complex, and the log*K* value for the equilibrium $[\mathrm{Cu}_2^{\mathrm{II}}(\mathbf{3})]^{4+} + \mathrm{Cl}^- \rightleftharpoons [\mathrm{Cu}_2^{\mathrm{II}}(\mathbf{3})(\mathrm{Cl})]^{3+}$ at pH 5.2, as obtained by a nonlinear least-squares procedure, is 3.98 ± 0.02. The limiting value of the absorption band at 410 nm is especially high ($\varepsilon = 12600\,\mathrm{M}^{-1}\,\mathrm{cm}^{-1}$). Analogous titration profiles were obtained for bromide and iodide ions: Br$^-$: $\log K = 3.01 \pm 0.01$, $\varepsilon = 10800\,\mathrm{M}^{-1}\,\mathrm{cm}^{-1}$; I$^-$: $\log K = 2.39 \pm 0.02$, $\varepsilon = 950\,\mathrm{M}^{-1}\,\mathrm{cm}^{-1}$. Surprisingly, titration with NaF did not cause any development of the yellow color. However,

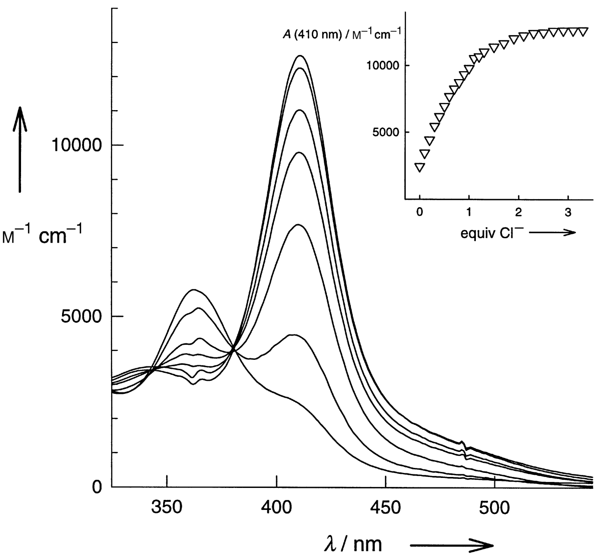

Figure 3. Titration of a solution containing $[\mathrm{Cu}^{\mathrm{II}}_2(\mathbf{3})]^{4+}$ with Cl^-, adjusted to pH 5.25 (0.05 M 2-morpholinoethanesulfonic acid buffer). The growing band centered at 410 nm corresponds to the formation of the inclusion complex $[\mathrm{Cu}^{\mathrm{II}}_2(\mathbf{3})(\mathrm{Cl})]^{3+}$. The titration profile in the inset gave a $\log K$ value of 3.98 ± 0.02 for the equilibrium $[\mathrm{Cu}^{\mathrm{II}}_2(\mathbf{3})]^{4+} + \mathrm{Cl}^- \rightleftharpoons [\mathrm{Cu}^{\mathrm{II}}_2(\mathbf{3})(\mathrm{Cl})]^{3+}$.

it must be considered that the absorption band has a halide-to-metal charge-transfer (CT) character, and its energy must therefore increase with increasing electronegativity of the halogen atom. It is possible that the CT transition for the complex $[\mathrm{Cu}^{\mathrm{II}}_2(\mathbf{3})(\mathrm{F})]^{3+}$, because of the high electronegativity of fluorine, is markedly shifted to lower wavelengths, in particular in the UV portion of the spectrum, where it is obscured by the intense amine-to-metal CT bands. Significant spectral modifications in the UV region were observed in the titration of the cryptate solution buffered at pH 5.2 with NaF. A saturation 1:1 profile was obtained, and the $\log K$ value was determined to be 3.20 ± 0.02.

The $\log K$ versus halide ion radius plot shown in Figure 4 reveals selectivity for chloride ions. The effect of anion size is rather moderate, ranging within an interval of 1.2 log units. However, the unique feature of the $[\mathrm{Cu}^{\mathrm{II}}_2(\mathbf{3})]^{4+}$ cryptate is its ability to accommodate anions of varying size and shape. Not only does it firmly encapsulate OH^- and halide ions, but it is also able to include linear triatomic anions such as N_3^- and NCS^-. In particular, when titrating a solution of $[\mathrm{Cu}^{\mathrm{II}}_2(\mathbf{3})]^{4+}$ adjusted to pH 5.2 with NaN_3, the pale blue solution became intense olive green, and the plot of the absorbance of the band which developed at 386 nm versus equivalents of N_3^- added indicated the formation of a 1:1 adduct with $\log K = 4.70 \pm 0.06$. The development of a CT band ($\varepsilon = 6100\,\mathrm{M}^{-1}\mathrm{cm}^{-1}$) as well as the 1:1 stoichiometry strongly suggest that the N_3^- ion is included within the cage. Similar behavior was observed with NCS^- ($\log K = 4.28 \pm 0.03$). Thus, it appears that the $[\mathrm{Cu}^{\mathrm{II}}_2(\mathbf{3})]^{4+}$ complex displays an extreme versatility, being able to contract and to expand its cavity to include (and form intense metal–ligand interactions with) anions of various sizes and shape, from the small hydroxide to the large thiocyanate ions. A closer inspection of available structural data suggests that the flexibility of $[\mathrm{Cu}^{\mathrm{II}}_2(\mathbf{3})]^{4+}$ is associated with the mobility of the 2,5-dimethylfuran spacers. In particular, the $\mathrm{Cu}^{\mathrm{II}} \cdots \mathrm{Cu}^{\mathrm{II}}$ distance in both $[\mathrm{Cu}^{\mathrm{II}}_2(\mathbf{3})\mathrm{Br}]^{3+}$ and $[\mathrm{Cu}^{\mathrm{II}}_2(\mathbf{3})\mathrm{OH}]^{3+}$ complexes can be varied at a low energy cost by adjusting the torsion angles along the chain arms adjacent to the 2,5-dimethylfuran spacer. Indeed, dramatic differences are observed in the NH-CH_2-C-O torsion angles in the two complexes: in the μ-bromo derivative the average value of such torsion angles is $-69(1)^\circ$ for the NH groups coordinated to one copper(II) center and $57(1)^\circ$ for the remaining NH groups; in the μ-hydroxo dicopper(II) complex the NH-CH_2-C-O torsion angles vary from $-68(1)$ to $76(1)^\circ$ for the NH groups coordinated to one copper(II) center, and from 75(1) to $-58(1)^\circ$ for the NH groups coordinated to the other copper(II) center. In other words, each NH-CH_2-C-O group behaves as a spring, which controls the length of the intermetallic cavity and can be operated through the variation of the magnitude of the corresponding dihedral angle. Apparently, an analogous spring mechanism can not be exhibited by the arms adjacent to the phenyl spacer in $[\mathrm{Cu}^{\mathrm{II}}_2(\mathbf{2})]^{4+}$, which does not contract its cavity and does not include monoatomic anions. It is possible that the $[\mathrm{Cu}^{\mathrm{II}}_2(\mathbf{3})]^{4+}$ cage can establish further unique bonding interactions which favor halide inclusion. In this regard, the intramolecular distances between C(4), O(1), and C(7) of each furan ring and the Br atom (O⋯Br 3.172(6)–3.212(6) Å, C⋯Br 3.339(8)–3.420(9) Å) are distinctly shorter than the sum of the van der Waals radii (3.37 and 3.55 Å, respectively). Hence, weak yet distinct interactions exist between the furan oxygen atoms and the encapsulated bromide ion in $[\mathrm{Cu}^{\mathrm{II}}_2(\mathbf{3})\mathrm{Br}]^{3+}$. These interactions cannot be established in the $[\mathrm{Cu}^{\mathrm{II}}_2(\mathbf{2})]^{4+}$ cage, which contains phenyl spacers, and may help to balance endothermic effects, if any, associated with cage contraction.

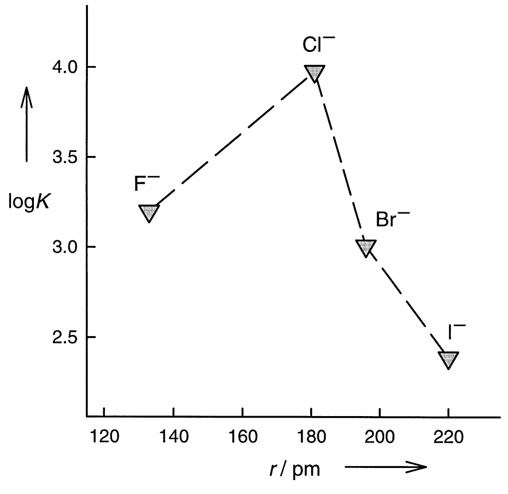

Figure 4. Selectivity pattern for the $[\mathrm{Cu}^{\mathrm{II}}_2(\mathbf{3})]^{4+} + \mathrm{X}^- \rightleftharpoons [\mathrm{Cu}^{\mathrm{II}}_2(\mathbf{3})(\mathrm{X})]^{3+}$ equilibrium (X^- = halide anion).

In conclusion, $[\mathrm{Cu}^{\mathrm{II}}_2(\mathbf{3})]^{4+}$ displays a special affinity towards halide ions, which are firmly encapsulated in a 1:1 stoichiometry. Halide inclusion can be detected visually by the appearance of an intense, bright yellow color, and instrumentally by the development of a very strong absorption band centered at 410–440 nm. In this regard, $[\mathrm{Cu}^{\mathrm{II}}_2(\mathbf{3})]^{4+}$ is an efficient colorimetric sensor of halide ions and joins the recently developed family of colorimetric sensors for inorganic anions.[13]

Experimental Section

Cage **3** was prepared as described.[7] Setup and procedures for spectrophotometric and potentiometric titration experiments have been reported elsewhere.[14] Equilibrium constants were determined by a nonlinear least-squares method.[15]

Received: March 27, 2000 [Z14901]

[1] C. J. Harding, F. E. Mabbs, E. J. L. MacInnes, V. McKee, J. Nelson, *J. Chem. Soc. Dalton Trans.* **1996**, 3227.

[2] L. Fabbrizzi, P. Pallavicini, A. Perotti, L. Parodi, A. Taglietti, *Inorg. Chim. Acta* **1995**, *238*, 5.

[3] R. J. Motekaitis, A. E. Martell, B. Dietrich, J.-M. Lehn, *Inorg. Chem.* **1984**, *23*, 1588.

[4] I. Murase, M. Mikuriya, H. Sonoda, S. Kida, *J. Chem. Soc. Chem. Commun.* **1984**, 692.

[5] A. Evers, R. D. Hancock, I. Murase, *Inorg. Chem.* **1986**, *25*, 2160.

[6] C. J. Harding, V. McKee, J. Nelson, Q. Lu, *J. Chem. Soc. Chem. Commun.* **1993**, 1768.

[7] Q. Lu, J.-M. Latour, C. J. Harding, N. Martin, D. J. Marrs, V. McKee, J. Nelson, *J. Chem. Soc. Dalton Trans.* **1994**, 1471.

[8] X-ray data for $[Cu^{II}_2(\mathbf{3})(Br)](ClO_4)_3$: a crystal of approximate dimensions $0.20 \times 0.35 \times 0.40$ mm was mounted on a glass rod protected from the air by a thin film of perfluoric oil. Diffraction data were collected on a Philips PW1100 diffractometer equipped with a normal focus 2.0-kW sealed-tube X-ray source operating at 50 kV and 20 mA with graphite-monochromated $Mo_{K\alpha}$ radiation ($\lambda = 0.71073$ Å). The unit cell parameters were determined by least-squares refinement on 30 $I_{hkl}(\theta, \kappa, \varphi)$ reflections found in a random search on the reciprocal lattice in the range $10 < \theta < 18°$. The intensities were determined by profile analysis[9] and corrected for Lorentzian and polarization effects. Scattering factors for neutral atoms and anomalous dispersion corrections for Cu were taken from the International Tables for X-Ray Crystallography.[10] The structure was solved by direct methods with SIR92[11] and then completed by cycles of Fourier ΔK and refined by full-matrix least-squares methods on F^2 by using SHELXL-96.[12] The parameters refined were the overall scale factor and the atomic coordinates and anisotropic thermal parameters for all non-hydrogen atoms. The hydrogen atoms were included in their calculated positions with the geometrical constraint d(X–H) = 0.96 Å and refined in the riding model. All calculations were carried out on a Digital Alfa255 workstation. Crystal data: $M_r = 1074.109$; monoclinic, space group $P2_1/c$, $a = 16.603(5)$, $b = 9.972(5)$, $c = 27.760$ (5) Å, $\beta = 101.26(2)°$, $V = 4508(3)$ Å^3, $Z = 4$, $\rho_{calcd} = 1.583$ g cm^{-3}, $F(000) = 2192$, $T = 293$ K. 6823 ($\pm h$, $+k$, $+l$) reflections were collected, of which 6205 were unique ($R_{int} = 0.04$) and 3329 observed ($F_o > 4\sigma(F_o)$). The refinement converged at $R1 = 0.058$, $wR2 = 0.17$ (all data), GOF: 0.86. Crystallographic data (excluding structure factors) for the structures reported in this paper have been deposited with the Cambridge Crystallographic Data Centre as supplementary publication no. CCDC-139472. Copies of the data can be obtained free of charge on application to CCDC, 12 Union Road, Cambridge CB21EZ, UK (fax: (+44)1223-336-033; e-mail: deposit@ccdc.cam.ac.uk).

[9] M. S. Lehmann, F. K. Larsen, *Acta Crystallogr. Sect. A* **1974**, *30*, 580.

[10] *International Tables for X-Ray Crystallography*, Kynoch, Birmingham, UK, **1974**.

[11] A. Altomare, M. C. Burla, M. Camalli, G. Cascarano, C. Giacovazzo, A. Guagliardi, G. Polidori, *J. Appl. Crystallogr.* **1994**, 435 (SIR92).

[12] G. M. Sheldrick, SHELX86, *Program for Crystal Structure Determination*, University of Göttingen, Germany, **1996**.

[13] C. B. Black, B. Andrioletti, A. C. Try, C. Ruiperez, J. L. Sessler, *J. Am. Chem. Soc.* **1999**, *121*, 10438; P. A. Gale, L. J. Twyman, C. I. Handlin, J. L. Sessler, *Chem. Commun.* **1999**, 1851; K. Niikura, A. P. Bisson, E. V. Anslyn, *J. Chem. Soc. Perkin Trans. 2* **1999**, 1111.

[14] V. Amendola, L. Fabbrizzi, C. Mangano, P. Pallavicini, A. Perotti, A. Taglietti, *J. Chem. Soc. Dalton Trans.* **2000**, 185.

[15] P. Gans, A. Sabatini, A. Vacca, *Talanta* **1996**, *43*, 1739–1753.

Unprecedented Expansion of the Pore Size and Volume of Periodic Mesoporous Silica**

Abdelhamid Sayari*

The synthesis of materials with designed pore structures is of paramount importance for many applications in areas such as catalysis, adsorption, and separation.[1] In designing such materials, several characteristics of the pore structure may be addressed, which include their shape, size, and connectivity. Since the discovery of the M41S periodic mesoporous silicas in the early 1990s,[2] a number of synthesis strategies to control their pore size have been developed. With only a few exceptions,[3, 4] all of the reported investigations dealt with MCM-41 silica whose pore structure consists of hexagonally packed unidimensional cylindrical channels (*p*6*mm*). In the latter case, the pore sizes may be adjusted from the lower end of the mesoporous range (about 2.0–2.5 nm) to well into the macroporous range. A summary of these approaches along with pertinent references is provided elsewhere.[5] In our earlier work,[6, 7] we found that treatment of as-synthesized 3.5 nm pore MCM-41 silica with long chain trialkylamines or *N*,*N*-dimethylalkylamines, typically at 100–130 °C for 2–3 days, increased the pore size to a maximum of about 11 nm. The pore volume also increased threefold from 0.8 to 2.4 cm^{3}g^{-1}. In this paper, we report an unprecedented pore size expansion from approximately 3.15 to 25 nm with conservation of the surface area and pore wall thickness.

The filled symbol in Figure 1 shows the nitrogen adsorption–desorption isotherm for MCM-41BT (BT = before treatment) with a sharp nitrogen condensation step at a

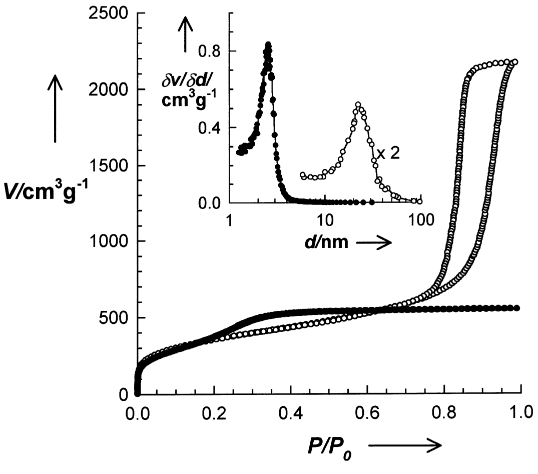

Figure 1. Nitrogen adsorption–desorption isotherms for MCM-41BT (●) and MCM-41AT (○). Inset: Corresponding PSDs (×2 indicates enhanced by a factor of 2).

---

[*] Prof. A. Sayari
Department of Chemical Engineering and CERPIC
Université Laval
Ste-Foy, Qc, G1K 7P4 (Canada)
Fax: (+1)418656-5993
E-mail: sayari@gch.ulaval.ca

[**] This was supported by the Natural Sciences and Engineering Research Council of Canada (NSERC). Thanks go to Y. Yang for technical help.